Estimation of the $S_{34}(0)$ S-factor for $^{3}He(\alpha, \gamma)^{7}Be$ reaction by using distorted wave born approximation and artificial neural network

Physica Scripta

PAPER

Estimation of the $S_{34}(0)$ S-factor for $^3He(\alpha, \gamma)^7Be$ reaction by using distorted wave born approximation and artificial neural network

G Kocak[1], **E Pasayigit**[1] and **S Akkoyun**[2]

[1] Department of Physics, Erciyes University, 38030, Kayseri, Turkey
[2] Department of Physics, Sivas Cumhuriyet University, 58140, Sivas, Turkey

E-mail: gkocak@erciyes.edu.tr

Keywords: artifical neural network, radiative capture reactions, fusion reactions

OPEN ACCESS

RECEIVED
27 March 2023

REVISED
2 August 2023

ACCEPTED FOR PUBLICATION
16 August 2023

PUBLISHED
6 September 2023

Abstract

The astrophysical S-factor and total cross-section of $^3He(\alpha, \gamma)^7Be$ radiative capture reaction are analyzed using the first-order distorted wave born approximation and artificial neural network. To make estimations of $S_{34}(0)$ at energies going to zero, we have used an artificial neural network model as a new approximation in this area. First, we obtain distorted wave born approximation results using the Gaussian and Woods-Saxon potentials. After, we evaluate artificial neural network approximation to analyze reaction observables of the $^3He(\alpha, \gamma)^7Be$ system. Our results show that artificial neural network model is a powerful candidate as an extrapolation model for astrophysical energies for estimating of the S-factor observable.

1. Introduction

Big Bang Nucleosynthesis (BBN) gives us one of the early universe's most precise and vital content. It has successfully explained reaction rates and abundances of very light elements, $A \leqslant 4$. However, recent observations of the metal-poor halo stars (MPHS) [1] have shown that the ^{6}Li and ^{7}Li abundances differ from BBN prediction. For $A \geqslant 4$ elements, the observed ^{7}Li abundance is about three times smaller and ^{6}Li abundance is 1000 times larger than the standard big bang nucleosynthesis (SBBN) [2, 3]. To explain this Li anomaly problem, the $^3He(\alpha, \gamma)^7Be$ reaction has immense importance, since the SBBN states that the $^3He(\alpha, \gamma)^7Be$ reaction and subsequent ^{7}Be decay are almost the primary sources to create ^{7}Li. Moreover, solar neutrino studies have taken great interest in nuclear astrophysics. The $^3He(\alpha, \gamma)^7Be$ reaction is crucial in determining the Sun's neutrino flux [4], since it is responsible for the second and third chains of the pp-cycle of hydrogen burning.

The cross section at solar energies is too small to be measured. Therefore, extrapolations are necessary to obtain reaction observables, like s-factor, cross sections, and reaction rates, at these energies. Various extrapolations methods have been developed to study these interactions in nuclear structure and reactions and to obtain observables. One of these methods is the Artificial Neural Networks (ANN) method, which has been used often in physics and other branches in recent years. In this method, the machine learning language algorithm is obtained by analogy with the structure and functions used to describe the neural transmission networks of the brain. The primary purpose here is to find an effective solution for situations where algorithmic equations are too dense. This method has recently become critical in data analysis in fields such as Nuclear Physics, High Energy Physics, Astrophysics, Biology, Chemistry, Meteorology and Geophysics [5]. In Nuclear Physics, with the help of the ANN model, in finding impact parameters in heavy-ion collisions [6–8], in statistical modeling of nuclear systematics, nuclear mass systematics development studies [9], determination of one and two proton separation energies, modeling of the systematics of β-decay half-lives [10] and creating a model for the estimation of nuclear charge radii [11], a remarkable amount of work is being done. The reason for using the ANN method in these studies and the most important advantage over other methods is that, unlike other extrapolation models, it does not need any equations or mathematical relations between the input and output data, it takes the earlier data, performs the operation and produces output. The ANN model can be used in non-linear equations to describe the relationship between input-output [5].

In the present study, we have calculated the total cross section and S-factor for the $^{3}He(\alpha,\ \gamma)^{7}Be$ reaction. Our ultimate goal is to present a new extrapolation approximation for the astrophysical reaction observables for solar energies. Also, to evaluate the reliability of ANN, we have made a comparison with the nuclear potential model. For this purpose, we have used distorted wave born approximation (DWBA) to study of $^{3}He(\alpha,\ \gamma)^{7}Be$ reaction. Also, to see the reliability of the ANN, we analysed $d(\alpha,\ \gamma)^{6}Li$ system at astrophysical energies as a different reaction in section 3.1. All analyses conducted within the framework of first-order distorted wave born approximation (DWBA). Section 2.1 introduces our models and phenomenological results for the $^{3}He(\alpha,\ \gamma)^{7}Be$ system. In section 2.2, we briefly explain the properties of ANN and in section 3, we give our results. Section 4 is devoted to the conclusion and summary.

2. Theory

2.1. DWBA model

The production of ^{7}Be is significant to the primordial big-bang nucleosynthesis at exceptionally low temperatures. However, studying the $^{3}He(\alpha,\gamma)^{7}Be$ system is challenging theoretically and experimentally due to the very low cross section of astrophysical energies. In this analysis, we have used the nuclear potential model to obtain the total cross section and S-factor for the $^{3}He(\alpha,\gamma)^{7}Be$ radiative capture reactions. There are either no open excited channels at astrophysically low energy for nuclear reactions or they are too weak. As a helpful approach, we have used the optical model potential to define the best potential model to get the reaction observables for given system. Using this potential, we have applied the first-order DWBA calculations for the $^{3}He(\alpha,\gamma)^{7}Be$ system to get reaction total cross section. The DWBA implicitly assumes that the elastic scattering is dominant while non-elastic contributions can be treated perturbatively.

The transitional amplitude for the DWBA to define inelastic scattering from initial channel (i) to final channel (f) is given by;

$$T_{fi}(k_f,\ k_i) = \int dr \chi_f^{(-)}(k_f,\ r)\langle \Phi_f | U(r,\ \beta)|\ \Phi_i\rangle \chi_i^{(+)}(k_i,\ r) \tag{1}$$

where k_i and k_f are wave numbers of entrance and exit channels, respectively. The distorted waves $\chi_i^{(+)}(k_i,\ r)$ and $\chi_f^{(-)}(k_f,\ r)$ give the relative motion between the interacting nuclei. The interaction potential is given by $U(r,\beta)$ and the β defines internal coordinates of the excited states. The cross section can be obtained by

$$\frac{d\sigma}{d\Omega}_{DWBA} \propto |T_{fi}|^2 \tag{2}$$

In our DWBA calculations, we have obtained the entrance channel potential for the ^{4}He+^{3}He by using the optical model potential as given below. There is no potential between the ^{7}Be and γ for the exit channel. The overlap wave function is defined by using ^{7}Be overlap for this system. Therefore, the spectroscopic factor for this reaction is chosen 1.

In our optical model, the total potential V_{total}(r) consists of

$$V_{total}(r) = V_{Nuclear}(r) + V_{Coulomb}(r) + V_{Cent.}(r). \tag{3}$$

The Coulomb and Centrifugal potentials are well-known in total potential. The Woods-Saxon volume and Gaussian shape has been used as the nuclear potential in our analyzes.

$$V_{WS}(r) = \frac{-V_0}{1 + \exp((r - R)/a)} \tag{4}$$

$$V_{Gaussian}(r) = -V_0 \exp(-((r - R)/a)^2) \tag{5}$$

where $R = r_0(A_P^{1/3}+A_T^{1/3})$. The Coulomb potential [12] due to a charge Z_Pe interacting with a charge Z_Te distributed uniformly over a sphere of radius R_c

$$V_{Coulomb}(r) = \frac{1}{4\pi\epsilon_\circ}\frac{Z_P Z_T e^2}{r}, \qquad r \geqslant R_c \tag{6}$$

$$= \frac{1}{4\pi\epsilon_\circ}\frac{Z_P Z_T e^2}{2R_c}\left(3 - \frac{r^2}{R_c^2}\right), \qquad r < R_c \tag{7}$$

where R_c is the Coulomb radius, and Z_P and Z_T denote the charges of the projectile P and the target nuclei T respectively.

The centrifugal potential is

$$V_{Centrifugal}(r) = \frac{\hbar^2\, l\,(l+1)}{2\,\mu\, r^2} \tag{8}$$

where μ is the reduced mass of the colliding pair. The Fresco code [13] has been used for all calculations.

The astrophysical S-Factor $S(E)$ is used for convenience, defined as follows:

$$S(E) = \sigma(E) E exp(2\pi\eta) \tag{9}$$

This $S(E)$ equation shows a strong energy dependence and η is given as the Sommerfeld parameter.

$$\eta = \frac{Z_1 Z_2 e^2}{\hbar}\sqrt{\frac{\mu}{2E}} \tag{10}$$

2.2. Artificial Neural Network model

Artificial Neural Network (ANN) is a mathematical model that imitates the functioning of the human brain and nervous system [14]. The structure of the model consists of neurons in a nerve cell and the connections that connect these neurons. The operating units in the model are neurons. Neurons are located in groups in three different layers. These layers are the input, hidden and output layers. Because of its layered structure, this type of ANN is called layered ANN. The independent variables of the problem are represented by neurons in the input layer. A separate neuron corresponds to each variable. In the output layer, the desired result of the problem, that is, the dependent variables takes place. The hidden layer, which is the layer in between, is a necessary layer for solving nonlinear problems. Communication and data transfer between neurons in the layers is achieved through connections with adjustable weights. The type of layered ANN in which data flows forward in one direction is called layered feed-forward ANN. The main goal in solving problems with this method is to determine the weight values of the connections between neurons, using a sample set of dependent and independent variables. Then, with the final weight values obtained, it is aimed to produce the desired outputs for each given input set.

The number of neurons in the input and output layers depends on the variety of data for the problem. In addition, there are no rules in determining the hidden layer and the number of neurons in this layer. The properties of the hidden layer are related to the nature of the problem, and the use of a single hidden layer is sufficient for solving almost all problems [15]. However, the number of hidden layer neurons for the problem that will give the best result can be determined after many trials. In the study planned to be carried out within the scope of this project proposal, the number of neurons in the output layer is 1, corresponding to the astrophysical S-Factor value. The neurons in the input layer will consist of independent variables that can affect the reaction cross-section. Because the use of some of these parameters will not affect the result and may even lead to bad results, and the absence of other parameters that are not included may also cause the result to be bad. One of the main pillars of the project proposal is to determine the appropriate input variables to get the right results. In the ANN method, this determination process does not depend on any physical formulation and will take place after many trials.

Each neuron in the hidden layer of the ANN has an input and an output. All incoming connections to a neuron provide data to that neuron. The addition function is a function that calculates the net input to that neuron. Typically, weighted aggregation is done. In this process, each input value to the neuron is multiplied by the weight value of the connection that transmits it, and the net input is calculated. Next, the net input to the neuron is processed, producing an output value corresponding to the input by this cell. This is done with the help of the activation function. The activation function can theoretically be any nonlinear function that behaves well. In general, this function is chosen as a sigmoid-type function in calculations.

ANN method is a tool that gives very successful results for both linear and nonlinear problems. The method basically consists of two main stages. These are the training and testing phases. All the data of the problem are divided into two separate groups for these stages, which is usually 80% for training and 20% for testing. In the first stage, the training stage, the first part of the data is given to the ANN, including both input and desired output values. By using this known data set, the weights between neurons are determined.

In this study, it is aimed to make S-factor estimations with ANN using nuclear reaction data. S-factor values were calculated using new data after 2000. In the establishment of the ANN model, the S-factor values corresponding to the Energy value as input data were estimated by ANN. 1 input, 1 output, and 1 hidden layer with 4 hidden layer neurons were used. Multilayer Perceptron was chosen from artificial intelligence methods. The activation function for hidden neurons can theoretically be a nonlinear function. In this study, the tangent hyperbolic activation function was used as given below.

Table 1. The calculated performance index for S-factor estimation during testing.

Performance	S
MSE	0.000326098
NMSE	0.071899417
MAE	0.015665494
Min. Abs Error	9.28885E-05
Max. Abs Error	0.032838677
r	0.971387998

Table 2. The calculated performance index for S-factor estimation during training.

Performance	S
MSE	0.000177433
NMSE	0.029226376
MAE	0.010580325
Min. Abs Error	4.53226E-05
Max. Abs Error	0.040934284
r	0.985278476

$$tanh = (e^{x} - e^{-x})/(e^{x} + e^{-x})$$

During the training phase, the first part of the data containing both input and desired output values is given to the ANN. The Levenberg-Marquardt algorithm was used for the training of the ANN. The Epoch number for training is set to 1000. In order to evaluate the Energy (E) and S-factor (S) parameters, both training and test phase performance were examined with different test and training data. With 105 data inputs with random data selection validation technique; 80 data were used for training and 25 data for testing. The training error value (minimun MSE) of approximately 0.004496462291 shows that the method is quite reliable. Tables 1 and 2 shows MSE (Mean Squared Error), NMSE (Normalized Mean Square Error), MAE (Mean Absolute Error), Min. Abs Error (Minimum Absolute Error), Max. Abs Error (Maximum Absolute Error), r (Linear Correlation Coefficient) for both training and test data was taken into account.

3. Results and discussions

As explained in section 1, the $^{3}He(\alpha, \gamma)^{7}Be$ reaction is significant for nuclear astrophysics studies and has been studied intensively. We can divide the experimental studies for this reaction into roughly before and after the year 2000. Before 2000, old experimental studies had insufficient experimental information like systematical errors. There are serious differences between the results of experimental studies even on the same energy range as given in Refs. [16–20]. These studies were generally carried out at energies under $E_{cm} = 1.5$ MeV. The modern experiments generally use prompt-γ ray [21–23], the measurement of the ^{7}Be activity [24–26] and the counting of ^{7}Be recoils [27] techniques. The energy ranges of these experiments change between $E_{cm} = 0.07$ and 3 MeV. There is a considerable difference in the absolute scale and the energy dependency of the S-factor from the results compared to earlier and new experiments.

Numerous theoretical models have been used to study $^{3}He(\alpha, \gamma)^{7}Be$ reaction such as the asymptotic normalization coefficient (ANC) technique [28, 29], R-matrix theory [30, 31], resonating group method [32] and potential models [33]. In this study, the theoretical analysis of the S-factor and total cross-sections of the $^{3}He(\alpha, \gamma)^{7}Be$ system at astrophysical energies has been performed based on the DWBA model. We have used Gaussian and Woods-Saxon type nuclear potentials of the $^{3}He(\alpha, \gamma)^{7}Be$ reaction as given in equations 4 and 5. The values of parameters used for the real and spin-orbit parts of the nuclear potentials are shown in table 3. To make a comparative study, we have presented the our theoretical results and experimental data in figure 1. At the same time, we compare our all theoretical results in figure 2. Inner part of figure 2, we presented the $S_{34}(0)$ estimation of our results.

Our analyses show that, the $E(1)$ transition is responsible for the main contribution of all energies as known from the literature [33]. We first used the Gaussian type potential [30] in our calculations. Unfortunately, we could not explain the experimental data at energies above 1MeV, as seen in figure 2. Then, we added the

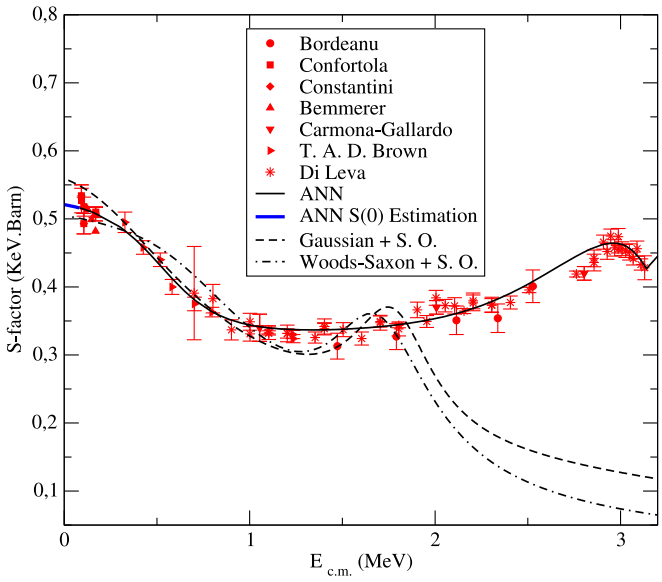

Figure 1. The S-factor results of $^{3}He(\alpha,\ \gamma)^{7}Be$ reaction with comparison our results and experimental data. The experimental data is obtained from [21–25, 27, 35].

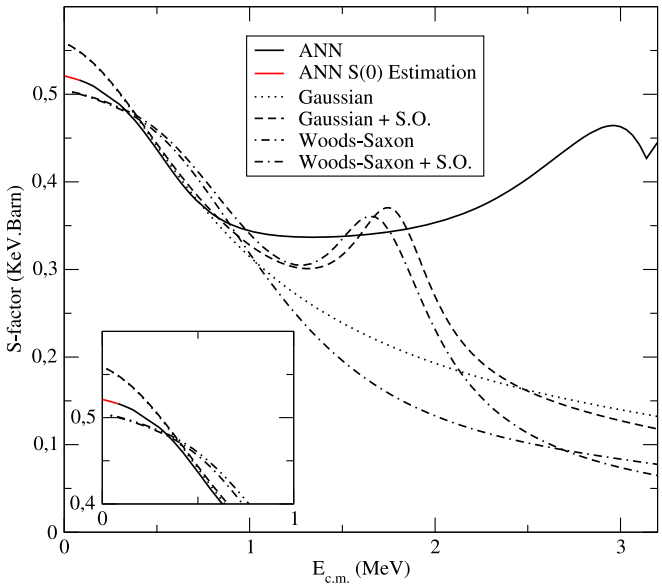

Figure 2. The S-factor results of $^{3}He(\alpha,\ \gamma)^{7}Be$ reaction for our DWBA and ANN calculations.

Table 3. The parameters of the real and spin-orbit potentials for the DWBA calculations.

Potential Type	V (MeV)	a (fm)	r_0 (fm)
Gaussian	300.5	1.120	0.850
Spin-Orbit for Gaussian	90.0	1.200	0.310
Woods-Saxon	88.0	1.105	0.635
Spin-Orbit for Woods-Saxon	53.0	1.000	0.290

spin-orbit potential and explained the experimental data up to around $E_{cm} = 1.7$ MeV. But there were serious differences between the theoretical results and the experimental data at energies bigger than 1.7 MeV. In addition, we obtained the reaction observables using Woods-Saxon potential. Nearly same behaviors were seen

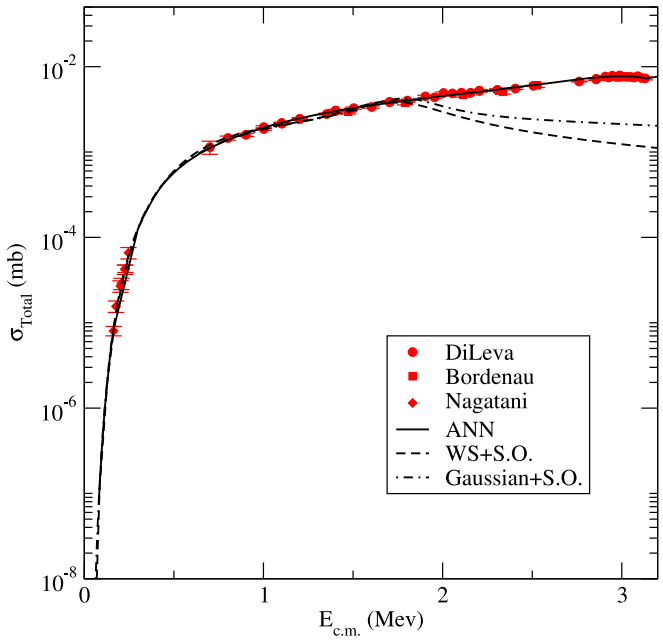

Figure 3. Comparison of the our best results for the $^3He(\alpha,\ \gamma)^7Be$ reaction total cross section. The experimental data are taken from [18, 25, 27].

Table 4. $S_{34}(0)$ values for different theoretical and experimental studies.

References	$S_{34}(0)$ (MeV.Barn)
Descouvement *et al* [30]	0.550 ± 0.017
Kajino [32]	0.540 ± 0.09
Angulo *et al* [39]	0.597 ± 0.019
Csoto and Langanke [40]	0.586 ± 0.018
Singh *et al* [41]	0.551 ± 0.022
Xu *et al* [42]	0.560 ± 0.05
Gaussian+S.O. this work	0.559
WS+S.O. this work	0.502
ANN this work	0.523

with the Gaussian potential. Our results are extremely sensitive to the potential parameters which used in these calculations. Therefore, it is quite difficult to explain all energies between $E_{cm} = 0$ and 3 MeV with same parameter set by using potential models. Recently, Li *et al* [31] obtained satisfactory results by using R-Matrix formalism. But this formalism needs very complex data sets to explain the S-factor in all energy ranges.

As a second part, we have evaluated the ANN model for the $^3He(\alpha,\ \gamma)^7Be$ system as given in section 2.2.

In our ANN calculations, the $^3He(\alpha,\ \gamma)^7Be$ reaction experimental data has been used as input data and estimated the energy going to zero as shown in inner part of figure 2. By using ANN model, the S-factor of the $^3He(\alpha,\ \gamma)^7Be$ system is explained perfectly not only below the $E_{cm} = 1.7$ MeV but also at the all energy region, and the phase and magnitude of the experimental data are reproduced very well. In table 4, we have presented our $S_{34}(0)$ results compared with the literature. As can be seen in table 4, our Gaussian and ANN results, except for the Woods-Saxon, are remarkably close to the average literature values. It shows us that the ANN model can be a very reliable extrapolation model for estimating $S_{34}(0)$ at astrophysical energies. We have also compared our best results for the total cross section in figure 3. Although our potential model results show good agreement at results less than $E_{cm} = 1.7$ MeV, it loses agreement with the experimental data at large energies. However, ANN results show excellent agreement in all energy regions.

3.1. $d(\alpha,\gamma)^6Li$ system

In this section, to test the validity of the ANN model, we have presented $d(\alpha,\ \gamma)^6Li$ system S-factor results in figure 4. ^6Li is one of the important element for the Li abundances problem [43, 44]. During the BBN period, this element was primarily synthesised using the direct capture $d(\alpha,\ \gamma)^6Li$ process. $d(\alpha,\gamma)^6Li$ reaction is very

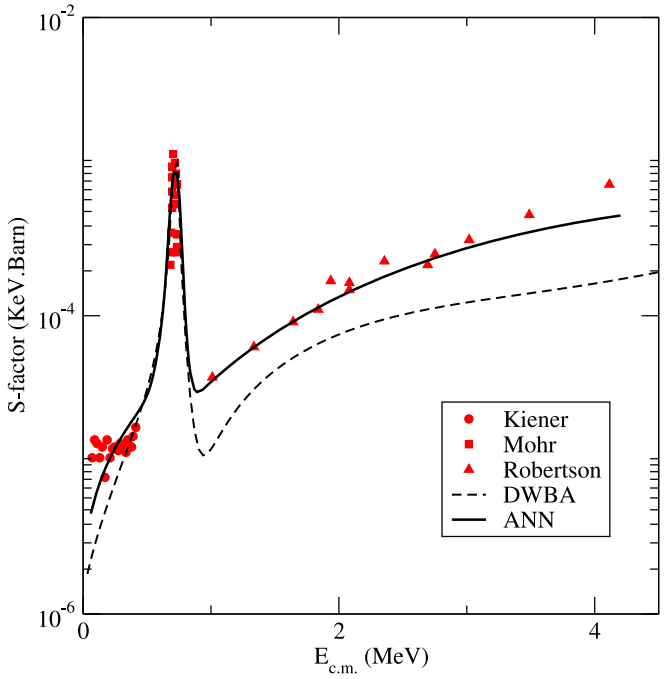

Figure 4. The S-factor results of $d(\alpha,\ \gamma)^6Li$ reaction with comparison our results and experimental data. The experimental data is obtained from [36–38].

different structure from the $^3He(\alpha,\gamma)^7Be$ reaction. It has resonance at $E_{cm} = 0.711$ MeV energy and has very low cross section [34]. Therefore, the predictions for $d(\alpha,\gamma)^6Li$ reaction observables are very uncertain due to both theoretical and experimental difficulties. In this study, firstly, we have examined DWBA model with potential set as given DWBA as can be seen from figure 4. To analyze this reaction, the nuclear potential parameters have taken V_0=39.70MeV, r_0=1.0 fm and a = 0.8 fm. In order to obtain the best fit, the $E(2)$ transition effect should be taken into account. Unfortunately, Our potential model failed to explain the experimental data at energies greater than $E_{cm} = 1$ MeV. On the other hand, we have conducted ANN model. The ANN model explained three different experimental data much better than DWBA model. This result is important in terms of showing us that the ANN model is a reliable method.

4. Summary and conclusions

In this paper, we have investigated the astrophysical S-factor and total cross-section of $^3He(\alpha,\gamma)^7Be$ reaction by using the first-order distorted wave born approximation and artificial neural network. First of all, the nuclear potential model have been used to analyze nuclear astrophysical observables. We have used the Gaussian and Woods-Saxon potentials in DWBA calculations, as given in section 2.1. The agreement between the theoretical results and the experimental data is reasonable until $E_{cm} = 1.7$ MeV. After the energies are bigger than $E_{cm} = 1.7$ MeV, our DWBA results do not explain experimental data. As given in figure 1, there are different type experimental data in different energy ranges. For of this reason, it is challenging to explain experimental data with the same potential set using a potential model. As a second part of this study, we have used the ANN model. It is clearly seen from figures 1–4 that our ANN results predicts perfectly the reaction observable, and reproduces the oscillatory structure of the S-factor and total cross-section data with correct phases and magnitudes. In addition, ANN prediction for the $S_{34}(0)$ is very compatible with the other data as seen in table 4. Our primary motivation in this study is to test reliability of the ANN results for the reaction obervables and $S_{34}(0)$ estimation in comparison with nuclear potential model. According to our results, the ANN model is extraordinary successful as an extrapolation method for astrophysical energies. It could be a powerful tool as an estimation method in a region where experimental data are not available. In our future studies, one of our main goals will be to test the reliability of the predictions made by the ANN model in places where there is no experimental data in comparison with theoretical models for different reactions.

Acknowledgments

This work was supported by the Erciyes University Scientific Research Projects Unit. Project Number: FBA-2022-11957.

Data availability statement

All data that support the findings of this study are included within the article (and any supplementary files).

ORCID iDs

G Kocak https://orcid.org/0000-0003-1784-7761
S Akkoyun https://orcid.org/0000-0002-8996-3385

References

[1] Asplund M, Lambert D L, Nissen P E, Primas F and Smith V V 2006 *Astrophys. J.* **644** 229
[2] Kusakabe M, Kajino T, Boyd R N, Yoshida T and Mathews G J 2007 *Phys. Rev.* D **76** 121302
[3] Spergel D N *et al* (WMAP) 2007 *Astrophys. J. Suppl.* **170** 377
[4] Bahcall J N, Pinsonneault M H and Basu S 2001 *Astrophys. J.* **555** 990–1012
[5] Negoita G A *et al* 2019 *Phys. Rev.* C **99** 054308
[6] David C, Freslier M and Aichelin J 1995 *Phys. Rev.* C **51** 1453–9
[7] Bass S A, Bischoff A, Maruhn J A, Stoecker H and Greiner W 1996 *Phys. Rev.* C **53** 2358–63
[8] Haddad F, Hagel K, Li J, Mdeiwayeh N, Natowitz J B, Wada R, Xiao B, David C, Freslier M and Aichelin J 1997 *Phys. Rev.* C **55** 1371–5
[9] Athanassopoulos S, Mavrommatis E, Gernoth K A and Clark J W 2004 *Nucl. Phys.* A **743** 222–35
[10] Costiris N J, Mavrommatis E, Gernoth K A and Clark J W 2009 *Phys. Rev.* C **80** 044332
[11] Akkoyun S, Bayram T, Kara S O and Sinan A 2013 *J. Phys.* G **40** 055106
[12] Satchler G R 1983 *Direct Nuclear Reactions* (Oxford: Oxford University Press)
Satchler G R 1980 *Introduction to Nuclear Reactions* (London: Macmillan)
[13] Thompson I J 1988 *Comput. Phys. Rept.* **7** 167
[14] Haykin S 1999 *Neural Networks: A Comprehensive Foundation* II edn (Englewood Cliffs, NJ: Prentice-Hall)
[15] Hornik K, Stinchcombe M and White H 1989 *Neural Netw.* **2** 359–66
[16] Holmgren H D and Johnston R L 1959 *Phys. Rev.* **113** 1556–9
[17] Parker P D and Kavanagh R W 1963 *Phys. Rev.* **131** 2578–82
[18] Nagatani K, Dwarakanath M R and Ashery D 1969 *Nucl. Phys.* A **128** 325–32
[19] Robertson R G H, Dyer P, Bowles T J, Brown R E, Jarmie N, Maggiore C J and Austin S M 1983 *Phys. Rev.* C **27** 11–7
[20] Osborne J L, Barnes C A, Kavanagh R W, Kremer R M, Mathews G J, Zyskind J L, Parker P D and Howard A J 1984 *Nucl. Phys.* A **419** 115–32
[21] Bemmerer D *et al* 2006 *Phys. Rev. Lett.* **97** 122502
[22] Brown T A D, Bordeanu C, Snover K A, Storm D W, Melconian D, Sallaska A L, Sjue S K L and Triambak S 2007 *Phys. Rev.* C **76** 055801
[23] Confortola F *et al* (LUNA) 2007 *Phys. Rev.* C **75** 065803
[24] Carmona-Gallardo M *et al* 2012 *Phys. Rev.* C **86** 032801
[25] Bordeanu C, Gyürky G, Halász Z, Szücs T, Kiss G G, Elekes Z, Farkas J, Fülöp Z and Somorjai E 2013 *Nucl. Phys.* A **908** 1–11
[26] Szücs T, Kiss G G, Gyürky G, Halász Z, Szegedi T N and Fülöp Z 2019 *Phys. Rev.* C **99** 055804
[27] Di Leva A *et al* 2009 *Phys. Rev. Lett.* **102** 232502
[28] Kiss G G *et al* 2020 *Phys. Lett.* B **807** 135606
[29] Mukhamedzhanov A M, Gagliardi C A and Tribble R E 2001 *Phys. Rev.* C **63** 024612
[30] Descouvemont P, Adahchour A, Angulo C, Coc A and Vangioni-Flam E 2004 *Atom. Data Nucl. Data Tabl.* **88** 203–36
[31] Li Y J, Li Z H, Wang Y B and Shen Y P 2022 *Nucl. Phys.* A **1022** 122444
[32] Kajino T 1986 *Nucl. Phys.* A **460** 559–80
[33] Mohr P, Avele H, Zwiebel R, Staudt G, Krauss H, Oberhammer H, Denker A, Hammer J W and Wolf G 1993 *Phys. Rev.* C **48** 1420–7
[34] Dapo H, Boztosun I, Kocak G and Balantekin A B 2012 *Phys. Rev.* C **85** 044602
[35] Costantini H *et al* 2008 *Nucl. Phys.* A **814** 144–58
[36] Kiener J, Gils H J, Rebel H, Zagromski S, Gsottschneider G, Heide N, Jelitto H, Wentz J and Baur G 1991 *Phys. Rev.* C **44** 2195–208
[37] Mohr P, Kolle V, Wilmes S, Atzrott U, Staudt G, Hammer J W, Krauss H and Oberhummer H 1994 *Phys. Rev.* C **50** 1543–9
[38] Robertson R G H, Dyer P, Warner R A, Melin R C, Bowles T J, McDonald A B, Ball G C, Davies W G and Earle E D 1981 *Phys. Rev. Lett.* **47** 1867–70
Robertson R G H, Dyer P, Warner R A, Melin R C, Bowles T J, McDonald A B, Ball G C, Davies W G and Earle E D 1995 *Phys. Rev. Lett.* **75** 4334 (erratum)
[39] Angulo C *et al* 1999 *Nucl. Phys.* A **656** 3–183
[40] Csoto A and Langanke K 2000 *Few Body Syst.* **29** 121–30
[41] Nara Singh B S, Hass M, Nir-El Y and Haquin G 2004 *Phys. Rev. Lett.* **93** 262503
[42] Xu Y, Takahashi K, Goriely S, Arnould M, Ohta M and Utsunomiya H 2013 *Nucl. Phys.* A **918** 61–169
[43] Reference Input Parameter Library (RIPL-3), www-nds.iaea.org/RIPL-3/.
[44] Cook J 1982 *Comput. Phys. Commun.* **25** 125